Lifespan of neurons is uncoupled from organismal lifespan

Lorenzo Magrassi[a,1], Ketty Leto[b,c], and Ferdinando Rossi[b,c]

[a]Dipartimento di Scienze Clinico–Chirurgiche Diagnostiche e Pediatriche, University of Pavia Fondazione Istituto di Cura a Carattere Scientifico (IRCCS) Policlinico San Matteo and Istituto di Genetica Molecolare–Consiglio Nazionale delle Ricerche, 27100 Pavia, Italy; [b]Department of Neuroscience, Neuroscience Institute of Turin, University of Turin, 10043 Orbassano, Italy; and [c]Neuroscience Institute of the Cavalieri Ottolenghi Foundation, University of Turin, 10125 Turin, Italy

Edited by Pasko Rakic, Yale University, New Haven, CT, and approved January 22, 2013 (received for review October 8, 2012)

Neurons in mammals do not undergo replicative aging, and, in absence of pathologic conditions, their lifespan is limited only by the maximum lifespan of the organism. Whether neuronal lifespan is determined by the strain-specific lifetime or can be extended beyond this limit is unknown. Here, we transplanted embryonic mouse cerebellar precursors into the developing brain of the longer-living Wistar rats. The donor cells integrated into the rat cerebellum developing into mature neurons while retaining mouse-specific morphometric traits. In their new environment, the grafted mouse neurons did not die at or before the maximum lifespan of their strain of origin but survived as long as 36 mo, doubling the average lifespan of the donor mice. Thus, the lifespan of neurons is not limited by the maximum lifespan of the donor organism, but continues when transplanted in a longer-living host.

Purkinje cells | dendrites

Median and maximum lifespan are characteristic of a species. However, whether cellular aging is the major determinant of organismal aging is still debated (1, 2). Replicative aging of continuously dividing cells is well characterized in vitro and in vivo (3). On the contrary, aging of terminally differentiated cells is less characterized and often equated with chronological aging (3). The latter is thought to include all age-related changes in a cell as a result of the stochastic accumulation of structural damage and their functional consequences. Most postmitotic neurons in the mammalian CNS survive aging (4), but specific differences in the lifespan of distinct neuronal populations have been described. Purkinje cells (PCs), the only output neuron of the cerebellar cortex, even in the absence of pathologic conditions, are progressively lost with aging in humans and mice (5, 6).

It is not known if a maximum lifespan exists for any postmitotic cells of mammals, including neurons. To address this issue, we exploited the differences in maximum lifespan of different strains of mice and rats. Although the two species have similar aging rates, and, in captivity, under optimal conditions, maximum lifespan of single outbreed individuals may reach 4 y (7), diverse strains of mice and rats differ significantly in their maximum lifespan, and these differences are genetically transmissible (8, 9). In utero, into the developing CNS of embryonic day (E) 15 embryos of Wistar rats, we transplanted cerebellar neuroglial precursors obtained from E12 mice embryos of mixed B6;129Sv background expressing EGFP in all cells (10). After birth of the transplanted rat embryos, we studied if the engrafted mouse cells survived for the entire life of the rat host.

Results

An outline of the experiment is presented in Fig. 1.

Recipient Rats Survived as Long as Two Times the Average Survival of Donor Mice. With the exception of animals electively perfused within 18 mo of life, the remaining graft recipient rats ($n = 59$; 86%) were let survive until moribund and unlikely to outlive longer than 48 h. Maximum survival of live-born recipient rats was 36 mo, whereas maximum survival of siblings of parents of donor mice embryos was 26 mo. Median survival for recipient rats that were not intentionally killed was 30 mo (minimum, 20 mo; maximum, 36 mo; $n = 59$ rats), whereas median survival of siblings of the parents of donor embryos was 18 mo (minimum, 6 mo; maximum, 26 mo; $n = 41$ mice). Survival curves of those mice and the recipient rats (Fig. 2*A*) were analyzed by the Kaplan–Meier method with log-rank test and found to differ significantly ($P < 0.0001$). Maximum lifespan of host rats and mice was also found to differ significantly ($P = 0.018$) by using the Fisher exact test applied to the proportion of animals alive in each group when 90% of the pooled populations had died (11).

Grafted Cells Developed into Cerebellar Neurons and Integrated into Host. Among recipient rats, 20 had EGFP-positive cells in the CNS, and 12 survived longer than 18 mo: the median survival of donor mice. Frequency, distribution and phenotypes of donor cells in the host brain (Figs. 2 and 3) were consistent with previous observations at shorter survival times (12, 13).

Integration of transplanted cells was not limited to the cerebellum; graft-derived cells were also found in the whole brainstem and, rarely, in the hemispheres. Ectopic and heterotopic locations of the transplanted cells are typical of the fetal grafting procedure and well documented at shorter survival times (12, 13). At all ages, EGFP-positive cells ectopically and orthotopically displayed typical features of different categories of mature cerebellar neurons (Figs. 2 *B*, *C*, and *E*–*G* and 3 *A*–*D*) and glia (Fig. 3*E*). When integrated orthotopically in the host cerebella, the donor cells always occupied characteristic positions and established morphologically appropriate relationships within the host tissue. At all ages, mouse PCs engrafted in the rat cerebella showed the typical laminar position, polarity, and orientation of their rat counterparts (Fig. 2 *B* and *E*–*G*). This was true even for granule cells that, after grafting, proliferated extensively, formed parallel fibers in the molecular layer, and settled in the internal granular layer (Figs. 2*B* and 3*A*).

Grafted PC Number Does Not Decrease with Aging. As we were studying if maximum survival of grafted mouse neurons corresponded to that of the donor mice or increased according to the host one, we focused our quantitative analyses on 13 rat brains containing multiple EGFP-positive PCs in the cerebellum. Under normal conditions, PCs would die with aging in a higher proportion (~40%) in mice (5, 14) than in rats (~11%) (15). Excluding from computations granule cells that proliferate after transplantation (12), the median number of EGFP-positive neurons

Author contributions: L.M., K.L., and F.R. designed research; L.M. and K.L. performed research; L.M., K.L., and F.R. analyzed data; and L.M., K.L., and F.R. wrote the paper.

The authors declare no conflict of interest.

This article is a PNAS Direct Submission.

[1]To whom correspondence should be addressed. E-mail: l.magrassi@smatteo.pv.it.

This article contains supporting information online at www.pnas.org/lookup/suppl/doi:10.1073/pnas.1217505110/-/DCSupplemental.

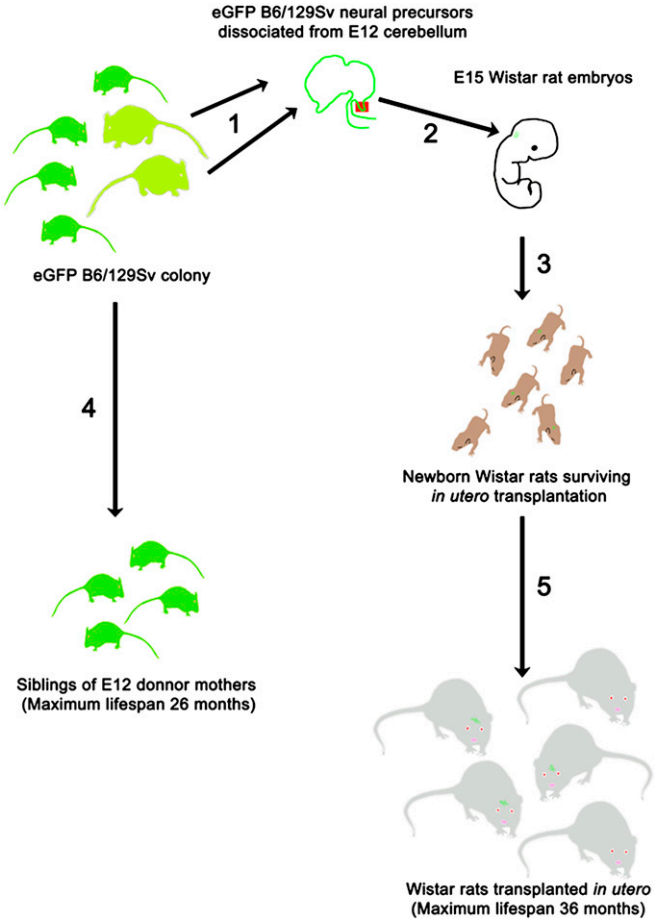

Fig. 1. Schematic outline of the experiment. (*1*) E12 fetuses were obtained from pregnant mothers in our colony of EGFP B6/129Sv mice, and the cerebellar primordium was dissected and mechanically dissociated into a single cell suspension. (*2*) A total of 5×10^4 E12 cerebellar precursor cells were injected through a glass microneedle into the developing cerebellum of E15 Wistar rats. All fetuses contained in the uterine horns were injected. (*3*) From our transplantation experiments, we obtained 69 live-born Wistar rats. (*4*) A total of 59 of these rats were allowed to survive until moribund and unlikely to survive for more than 2 d; at that time, they were perfused, and their cerebella and brainstem were collected for histological processing.

in rats perfused within 18 mo was 61 (range, 7–465; $n = 6$ rats) and the median number of PCs was 26 (range, 6–196; $n = 6$ rats). In rats surviving 19 to 36 mo, the median number of EGFP-labeled neurons was 36 (range, 13–333; $n = 7$ rats), whereas the median number of PCs was 28 (range, 7–209; $n = 7$ rats). The average number of EGFP-positive PCs in each transplant did not decrease with aging (Fig. 2*D*). The average number of EGFP-positive PCs was actually slightly higher in rats perfused after 18 mo (76 ± 86.96) than in younger rats (51 ± 72.07), although this difference was not significant ($P = 0.5968$, unpaired t test; and $P = 0.5338$, Mann–Whitney test).

Graft-Derived PCs Retained Mouse Morphometric Characteristics. In line with our observations on younger hosts (12, 13), mouse PCs grafted into rat cerebella maintained at, all survival times, their typical laminar position, polarity, and orientation (Fig. 2 *B* and *E*–*G*). Despite appropriate integration, grafted mouse cells retained morphometric traits characteristics of mouse PCs (Figs. 2*B* and 4 *B*–*E*). They were smaller than the surrounding rat PCs, and their dendrites did not reach the top of the molecular layer (Fig. 4*B*).

The area of the soma of mouse PCs was, on average, 245.56 μm^2 (±78.19; $n = 160$; Fig. 3*D*) whereas that of host rat cells was 354.59 (±74.16; $n = 308$; Figs. 2*D* and 4*C*). The span of the dendritic arbor of grafted mouse PCs measured perpendicularly to the cell body was 87.82 μm (±42.98; $n = 193$; Fig. 2*E*), whereas dendrites of the surrounding rat PCs reached 178.76 μm (±45.95; $n = 308$; Figs. 2*E* and 4*D*). When located in extracerebellar sites, EGFP-positive cells maintained cerebellar-specific traits that allowed their reliable identification. Ectopic PCs (Fig. 2*C*) also retained mouse morphometric traits, with an average soma area of 225.41 μm^2 (±66.46; $n = 198$) and dendritic span of 60.88 μm (±26.42; $n = 213$). Means and medians of areas and dendritic span of grafted mouse PCs were significantly different ($P < 0.0001$, unpaired t test and Mann–Whitney test) from those of the rat hosts, whereas the dimensions of grafted mouse PCs were similar to those reported for PCs in B6 mice, one of the parental strains of our mice (16). To investigate if the different dimensions reflected species-specific features or were induced by xenotransplantation, we grafted mouse and rat cerebellar precursors into conspecific embryos in utero. One month after grafting, the average soma area and the average dendritic span of transplanted rat PCs were 346.64 μm^2 (±89.36; $n = 22$) and 162.07 μm (±35.64; $n = 26$), respectively, values not significantly different from the respective values of 321.89 μm^2 (±56.52; $n = 43$) and 160.41 μm (±15.98; $n = 27$) of the host rat PC. Contrary to grafted mouse PCs (Fig. 4*B*), the dendritic arbor of grafted rat PCs reached the top of the molecular layer (Fig. 4*A*) and was morphometrically undistinguishable from those of the surrounding host PC. Similarly, 1 mo following transplantation of E12 mouse PCs into E15 Friend leukemia Virus 1B (FVB) mouse embryos, the area of their soma and their dendritic span were 257.38 μm^2 (±34.20; $n = 11$) and 102.48 μm (±38.05; $n = 10$), respectively, values significantly smaller than those of the rat cells reported earlier (unpaired t test and Mann–Whitney test, $P \leq 0.0003$) but not significantly different from those of the surrounding mouse PCs.

Grafted PCs Lose Dendritic Spines with Aging. Although the number of surviving PCs did not change with aging, we found a significant decrease in spine density on their dendrites, as previously described in aging rats (17). The median number of spines every 5 μm of dendritic length of the grafted PCs decreased from 14 (range, 10–20; $n = 134$ samples from six different PCs) at 1 mo to 9 (range, 5–15; $n = 269$ samples from nine different PCs) at 18 mo and down to 6 (range, 4–11; $n = 233$ samples from 13 different PCs) in rats surviving 36 mo (Fig. 4 *E* and *F*).

Discussion

Our results suggest that mouse cerebellar neural and glial precursors, xenotransplanted into the rat CNS, integrate into the host tissue and differentiate, maintaining species-specific morphometric traits, but survive as long as the surrounding host rat neurons, doubling their expected average survival in the mouse. Alternative explanations that might posit the generation of stable mouse–rat heterokaryons after cell fusion as described for PCs after bone marrow grafting (18, 19), are unlikely because EGFP-labeled PCs maintained mouse morphometric traits, were uninucleated (Fig. S1), and showed appropriate developmental stages in rats killed a few days after grafting (Fig. S2). Moreover, at all ages, we also found fluorescent PCs ectopically scattered along the brainstem. In normal rats, ectopic PCs are extremely rare and restricted to the dorsal cochlear nucleus (20, 21), whereas ectopic PCs are common after in utero transplantation of PC precursors (12), further indicating that the EGFP-labeled PCs did not result from fusion of grafted cells with host PCs. Direct transfer of EGFP to host PCs from microglial cells loaded with fluorescent cellular debris generated by the transplantation procedure, as described by Ackman et al. (22) in pyramidal neurons during

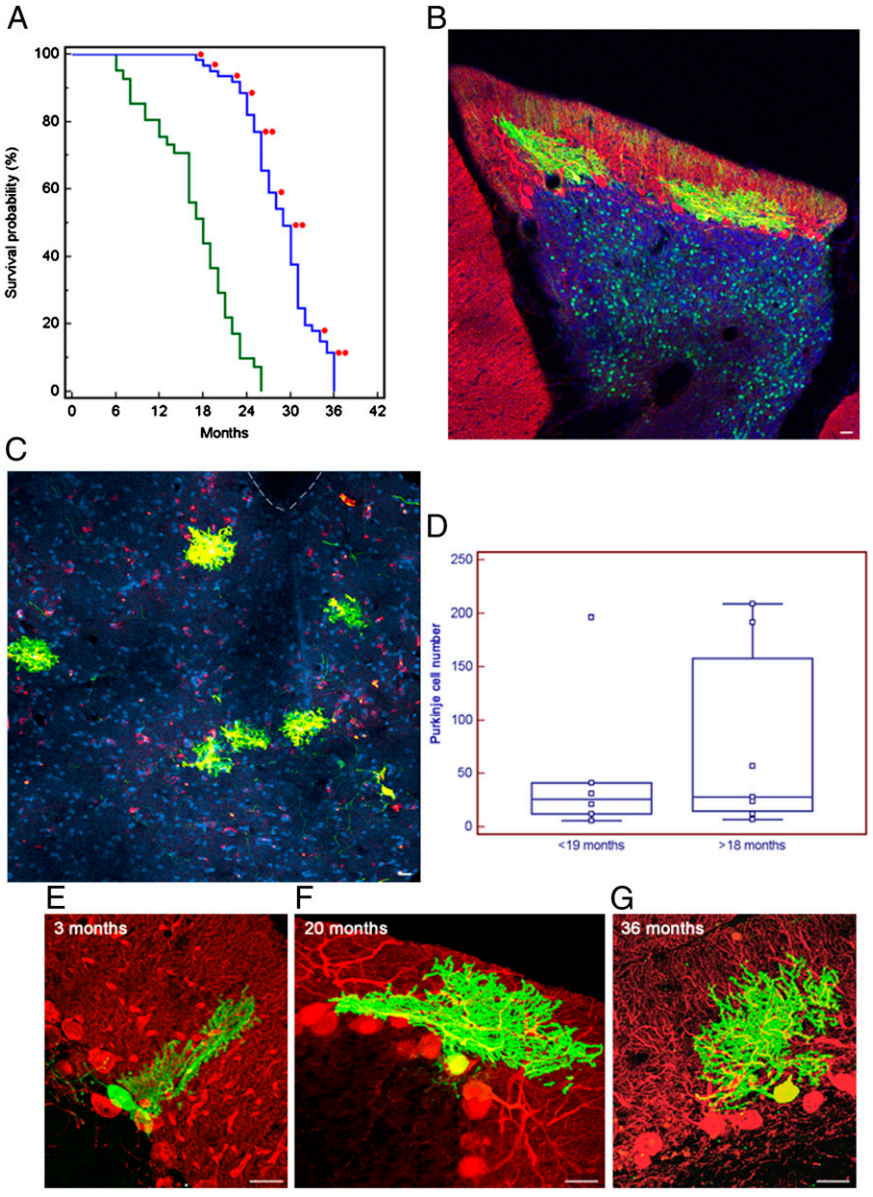

Fig. 2. Developing mouse cerebellar neurons transplanted in utero into the developing rat CNS integrate and survive to the rat host maximum lifespan, doubling the average lifespan of the neurons in the donor mice strain. (*A*) Kaplan–Meier plot showing lifespan of siblings of donor mice and rat host. Rats perfused electively were excluded from the survival curve. Each red dot indicates a transplanted rat in which we found mouse cells. (*B*) Parasagittal section from confocal microscopy of a 20-mo-old rat cerebellum. Fluorescences are as follows: EGFP (green), anti-calbindin antibody (red), overlapping fluorescence (yellow), and DAPI nuclear staining (blue). Two grafted mouse PCs are integrated in the host PC and molecular layers, and granular cells of mouse origin are visible in the granular layer (asterisks). (Scale bar: 25 μm.) (*C*) Same as Fig. 1*A*, but coronal section of the brainstem and fourth ventricle of a 36-mo-old graft, in which six ectopic calbindin/EGFP-positive PCs are visible in the brainstem outside the dorsal cochlear nucleus. Interrupted line indicates the ventricle. (Scale bar: 50 μm.) (*D*) Plot of the number of PCs found in the transplanted animals at different ages (<19 mo, rats perfused before 19 mo of age; >18 mo, rats perfused after 18 mo to 36 mo of age). Each square represents a single animal: <19 mo, $n = 6$; >18 mo, $n = 7$. Differences in mean and median number of PCs in the two groups were not significant ($P = 0.5968$, unpaired Student t test; $P = 0.5338$, Mann–Whitney test). Horizontal line indicates the median; central box encloses values from the lower to upper quartile; vertical line extends from the minimum to the maximum value, excluding outside and far out values. (*E–G*) Parasagittal sections as in Fig. 1*A* but without DAPI. Rat cerebella at 3, 20, and 36 mo of age showing mouse-derived PCs. The span of mouse PC dendrite did not reach the top of the host molecular layer and remained approximately the same at all survival times. (Scale bar: 25 μm.)

acute experiments involving retroviruses, is also not an acceptable explanation for the lifelong presence of EGFP-containing PCs, as EGFP after transfer persists less than 2 wk (22). All the aforementioned considerations indicate that EGFP-containing PCs found at all ages in the transplanted rats are mouse PCs integrated into the host CNS. Contrary to the long-term results of xenotransplantation of quail neural primordia into chicken embryos, which developed, after a few months, an immunomediated demyelinating disease (23), we did not detect any sign of rejection of the grafted mouse cells. In our experiment, the absence of grafted cells outside the recipient CNS, where they would have induced an immune response (24), and species-specific differences in the immune system may explain the undisturbed survival of our cells. Aging in CNS is accompanied by reduced synaptic connectivity, but not by generalized neuronal loss (25). PCs are an exception, with a documented age-related loss in several mammalian species (5, 6, 15). PC loss may be as much as 40% in mice (5, 14) but is lower in rats (10%) (15) or is even absent in specific cerebellar lobules (26). In our transplants, the number of mouse PCs did not decrease in older rats, further suggesting that lifespan of the transplanted neurons was not dictated by their mouse genetic background, but by the rat microenvironment. In mice, age-dependent loss of PCs has been related to a decrease in concentration of circulating sex steroid hormones (27). However, the increased survival of mouse PCs after xenotransplantation is unlikely to depend on differences in sex steroid, as levels and oscillations of those hormones are similar in aging mice and rats (28, 29).

The maximum survival of transplant-bearing rats fed ad libitum and maintained under clean but not "pathogen-free" conditions doubled the mean lifespan of transplanted mouse neurons, increasing their maximum lifespan by 38%. Those increases are larger than the relative increases in organismal lifespan induced in mice by dietary (30), pharmacologic (31), and most genetic manipulations (32), even though, rarely, individual mice of other strains and lines may reach lifespans comparable to those of our longest-surviving rats (9, 33). Despite the increase in PC survival induced by xenotransplantation, the expected age-related loss of connectivity (25), as shown by the progressive decrease in the number of dendritic spines (17), did not cease. This further indicates that the transplanted mouse PCs are well integrated in the rat cerebellum and undergo the same changes induced by aging in their rat counterpart.

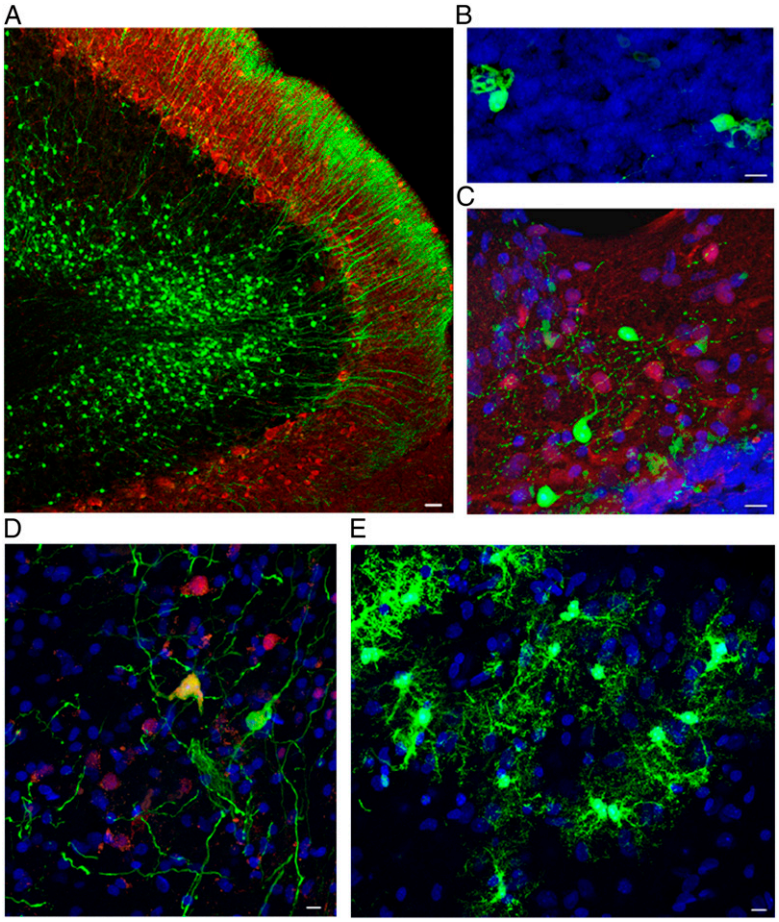

Fig. 3. Together with PCs, all other neural and glial phenotypes derived from transplanted mouse cerebellar precursors survived, as long as the host rat did. All of the following examples are from rats surviving beyond 20 mo. Confocal images of sagittal sections of brainstem and cerebellum of transplant-bearing rats. (*A*) EGFP-positive granule cells engrafted in the recipient internal granular layer. The axons of these neurons (parallel fibers) can be seen in the overlying molecular layer. Green indicates EGFP; red indicates calbindin. (Scale bar: 25 μm.) (*B*) Unipolar brush cells in the host granular layer displaying the typical dendritic structure. Green indicates EGFP; blue indicates DAPI nuclear staining. (Scale bar: 10 μm.) (*C*) Molecular layer interneurons and basket and stellate cells located in the recipient molecular layer of the cerebellar cortex. Green indicates EGFP; red indicates parvalbumin; blue indicates DAPI nuclear staining. (Scale bar: 10 μm.) (*D*) Neurons in the deep nuclei show multipolar morphology and express NeuN. Green indicates EGFP; red indicates NeuN; blue indicates DAPI nuclear staining. (Scale bar: 10 μm.) (*E*) Astrocytes scattered through the cerebellar white matter. Green indicates EGFP; blue indicates DAPI nuclear staining. (Scale bar: 10 μm.)

Our results suggest that neuronal survival and aging are coincidental but separable processes, thus increasing our hope that extending organismal lifespan by dietary, behavioral, and pharmacologic interventions will not necessarily result in a neuronally depleted brain.

Materials and Methods

Animals. Animals were maintained and handled, and all experimental manipulation performed, in agreement with the institutional guidelines of our institutions, the University of Pavia and the University of Turin. Our institutional guidelines comply with the National Institutes of Health guidelines, the requirements of the European Communities Council Directive (86/609/EEC), and the Italian law for care and use of experimental animals (DL116/92).

The colony of fluorescent mice was generated in 1999 by crossing a female TgN(beta-act-EGFP)01Obs (34) and a male B6.129S7-Gtrosa26 (35). Initially, the offspring were individually checked for EGFP expression, and only the siblings with fluorescence were crossed again. Selection of siblings and crossing was repeated at each generation until all siblings showed fluorescence; thereafter, we maintained the colony by sibling crossing without further need to select the offspring with fluorescence (10). During the entire length of the experiment (2007–2011), siblings of the female mice crossed to obtain the embryos dissected for harvesting cells for transplantation were allowed to survive until death or euthanasia when moribund and unlikely to survive for more than 48 h, and a survival curve was obtained. E14 transgenic rat embryos overexpressing EGFP under the control of the human CMV enhancer and β-actin promoter were obtained from a colony maintained in our laboratory (founders were a gift from M. Okabe, Osaka University, Osaka, Japan) (36). Time pregnant Wistar rats and FVB mice were obtained from Harlan. Mice and rat colonies were maintained at 21 °C to 23 °C in four of six mice or one of three rats per cage without microbiological barriers in a clean animal house environment, with access restricted to authorized personnel only. Mouse and rats colonies were routinely (twice per year) monitored for common pathogens; cages and bedding were changed every week for mice and two times per week for rats. Mice had ad libitum access to water and standard complete pelleted diet (Harlan).

Transplantation. All surgical procedures were carried out under deep general anesthesia obtained by i.p. injection of ketamine (100 mg/kg; Ketavet; Bayer) supplemented by diazepam (2.5 mg/kg; Roche).

Heterospecific transplantations: Mouse to rat. In utero, into the CNS of E15 Wistar rat fetuses, we transplanted 10^4 cells obtained by mechanical dissection of the cerebellar primordia of E12 mice embryos of mixed B6;129Sv background expressing EGFP in all neurons (10). Transplantation techniques and dissociation procedures were as previously described (12, 37). An outline of the experiment is presented in Fig. 1. A total of 69 live-born graft recipient Wistar rats entered the experiment; of these, 10 were perfused before 18 mo and 59 were perfused after 18 mo of life. Data obtained from four of the rats perfused before 18 mo were also included in an unrelated study.

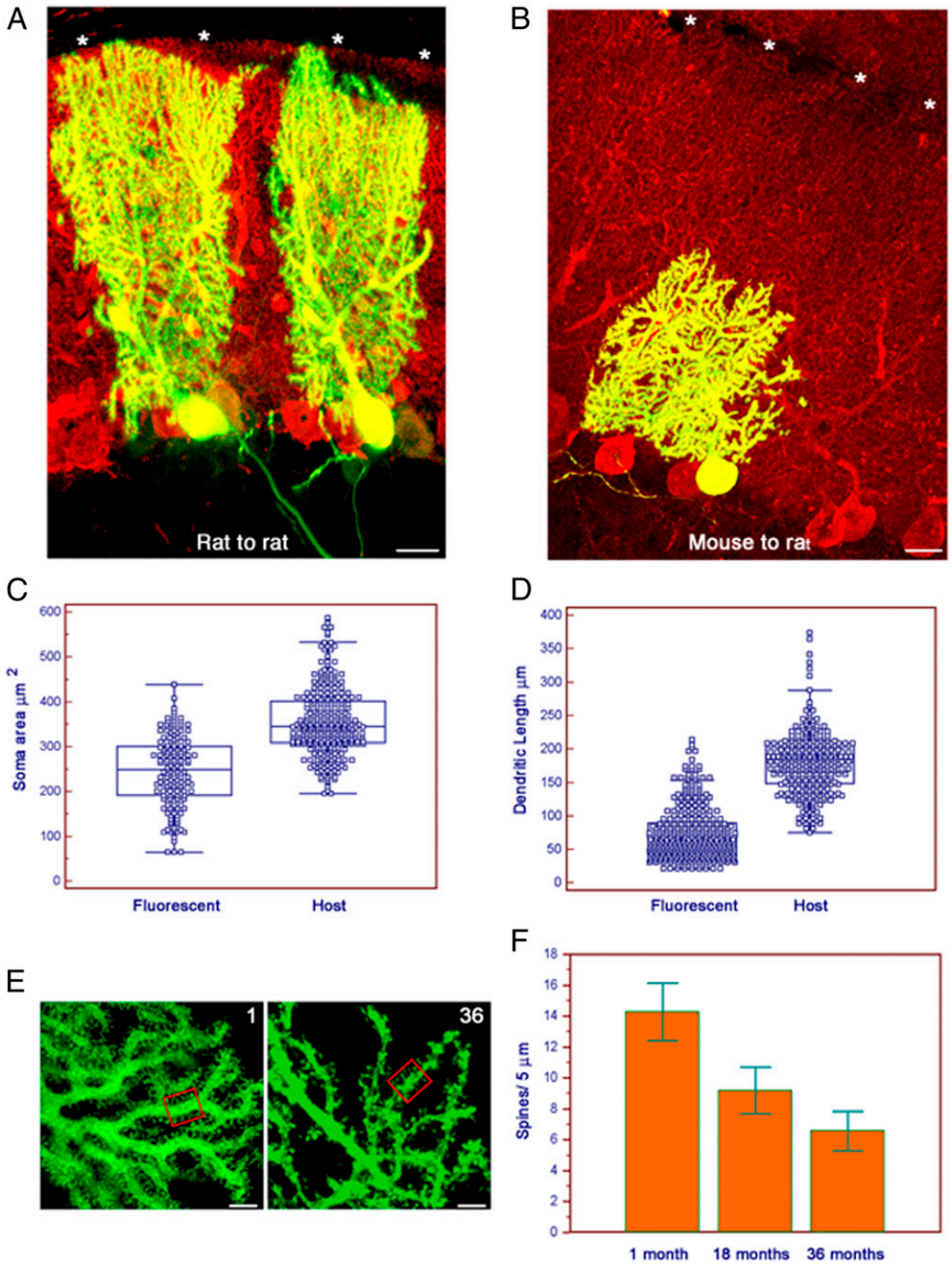

Fig. 4. Mouse PCs retain mouse morphometric characteristics when integrated in the rat cerebellum and undergo a progressive loss of dendritic spines with aging. (*A*) Parasagittal section stained as in Fig. 1*E*. Two rat PCs at 35 d after in utero transplantation into rat cerebellum. The grafted rat PC extends its dendrite to the top of the molecular layer (asterisks). (Scale bar: 25 μm.) (*B*) Same as Fig. 2*A* but mouse PC 35 d after in utero transplantation into rat cerebellum. Despite a fully mature PC phenotype, the mouse cell did not reach the top of the rat molecular layer (asterisks). (Scale bar: 25 μm.) (*C*) Plot of the areas of the PC soma of grafted mouse (marked as "M") and host rat ("R") cells. Cells were in the cerebellum. All survival times are pooled. Each square represents a single area (mouse, $n = 160$; rat, $n = 308$). The mean difference of 109.03 μm^2 was highly significant (95% CI of difference, 94.56–123.50; $P < 0.0001$, unpaired Student *t* test and Mann–Whitney test). Lines and boxes are as in Fig. 1*D*. (*D*) Plot of the span of grafted mouse ("M") and host rat ("R") PC dendrites. Cells and times are as in Fig. 2*C*. Each square represents a single dendrite (mouse, $n = 193$; rat, $n = 308$). The mean difference of 90.94 μm was highly significant (95% CI, 82.85–99.03; $P < 0.0001$, unpaired Student *t* test and Mann–Whitney test). Lines and boxes are as in Fig. 1*D*. (*E*) Grafted mouse PC dendrites at 1 and 36 mo of age. We counted by optical sectioning all spines contained in randomly selected 5 μm of dendrite. (Scale bar and boxes: 5 μm.) (*F*) Histogram demonstrating progressive decrease in average number of spines at 1, 18, and 36 mo of age. Error bars indicate SDs.

Isospecific transplantations. Mouse to mouse. A total of 10^4 of the same cells used for mouse-to-rat transplantations were transplanted in utero into E15 FVB mouse fetuses at a developmental stage equivalent to E15 in the rat. After transplantation, we obtained 11 live-born graft recipient FVB mice, and they were all perfused before 18 mo.

Rat to rat. The same number of cells described in the two previous experimental paradigms, but derived from E14 transgenic rat embryos (36)—a developmental stage equivalent to E12 in the mouse—were grafted in utero into the cerebellum of E15 Wistar rat fetuses. We obtained 37 live-born graft recipient Wistar rats; of these, three were perfused before 18 mo and 34 were perfused after 18 mo of life.

Histology and Data Collection. ***Harvesting and processing of the tissues.*** Animals were killed by transcardiac perfusion of 500 mL of 4% (wt/vol) paraformaldehyde

(Sigma-Aldrich) in 0.12 M phosphate buffer, pH 7.2 to 7.4, under deep general anesthesia, obtained by supplementing the previously described anesthetic protocol used for surgery with an euthanizing dose of ketamine after induction of anesthesia and before perfusion.

After perfusions, the brains were removed, stored overnight in the same fixative agent at 4 °C, and finally transferred in 30% sucrose in 0.12 M phosphate buffer. The fixed cerebella were placed in 30% sucrose in PBS solution overnight, embedded in Tissue-Tek optimum cutting temperature compound (VWR International), and serially cut on a cryostat at 30 μm. Cryostat sections were immunohistochemically stained with anti-calbindin antibodies to label PCs (1:1500; monoclonal or polyclonal; Swant), anti-parvalbumin (1:1,500; monoclonal; Swant) for molecular layer interneurons, anti-NeuN (1:500; monoclonal; Chemicon) for deep nuclei interneurons, and anti-GFP antibodies (1:700; polyclonal or monoclonal; Life Technologies) to enhance the GFP fluorescent signal of transplant-derived cells. Incubation of cerebellar slices with primary antibodies was made overnight at room temperature in PBS solution with 1.5% normal serum and 0.25% Triton X-100. The sections were then exposed for 1 h at room temperature to secondary biotinylated antibodies followed by a solution of streptavidin Texas red conjugate (1:200; Invitrogen) or fluoresceinated secondary antibody (1:200; Vector Laboratories). Nuclei were counterstained with DAPI (Sigma-Aldrich). The sections were mounted on microscope slides with Tris-glycerol supplemented with 10% Mowiol (Calbiochem) to reduce fading of fluorescence.

Microscopical analysis. By systematic inspection of all serial sections under a Zeiss Axiophot light microscope equipped with a Nikon DS-5M digital camera, or a Fluoview 300 microscope confocal microscope (Olympus), we traced and counted all EGFP-positive cells present in the cerebellum and brainstem of the transplanted animals. Positive cells were classified on the basis of their specific phenotype and antigenic reactivity. Quantitative and morphometric evaluations were made using the Neurolucida software (MicroBrightField) connected to an E-800 microscope (Nikon) via a color CCD camera. Photoshop 8.0 (Adobe Systems) was used to adjust image contrast and assemble the final plates.

Measurement of PC dendritic span. We measured the maximum dendritic span in sagittal sections by measuring, in Neurolucida software, the perpendicular distance between the plane of origin of the principal dendrite from the PC soma and the end of the dendritic arbor in the molecular layer.

Spine counts. In a randomly selected subset of mouse PCs found after 1, 18, and 36 mo of survival after heterospecific grafting, we analyzed dendritic spines present in the entire dendritic arbor by confocal optical sectioning. Spine numbers were obtained by counting all spines present in 134, 269, and 223 randomly selected 5-μm segments of mouse PC dendrites, respectively, in 6, 9, and 13 different PCs. Spine counts were performed in at least three animals for the different survival times.

Statistical Analysis. Survival was calculated by using the date each mouse was found dead or moribund. For rats surviving > 18 mo, we used the date of perfusion that corresponded to the day when the rat was considered unable to survive for more than 2 d. Statistical significance was assessed by parametric (unpaired Student *t* test) and nonparametric (Mann–Whitney test) methods when two groups were compared. Statistical analyses and survival curves were calculated by using MedCalc software.

ACKNOWLEDGMENTS. We thank P. A. Lawrence and E. Arbustini for helpful comments on the manuscript and M. Okabe (Osaka University) for the generous gift of transgenic mouse and rats expressing EGFP in all CNS cells. This work was supported by grants from Fondazione Istituto di Ricerca e Cura a Carattere Scientifico Policlinico San Matteo–Ricerca Corrente (to L.M.), Ministero dell'Università e della Ricerca–Progetti di Rilevante Interesse Nazionale 2009 (to F.R.), Compagnia di San Paolo [Gabagen Project 2010 (to F.R.)], and Ministero dell'Università e della Ricerca Fondo per l'Incentivazione della Ricerca di Base Research Grant RBFR10A01S (to K.L.).

1. Jeyapalan J-C, Sedivy J-M (2008) Cellular senescence and organismal aging. *Mech Ageing Dev* 129(7-8):467–474.
2. Rodier F, Campisi J (2011) Four faces of cellular senescence. *J Cell Biol* 192(4):547–556.
3. Rando T-A, Chang H-Y (2012) Aging, rejuvenation, and epigenetic reprogramming: Resetting the aging clock. *Cell* 148(1-2):46–57.
4. Esiri M-M (2007) Ageing and the brain. *J Pathol* 211(2):181–187.
5. Andersen B-B, Gundersen H-J-G, Pakkenberg B (2003) Aging of the human cerebellum: A stereological study. *J Comp Neurol* 466(3):356–365.
6. Woodruff-Pak D-S, et al. (2010) Differential effects and rates of normal aging in cerebellum and hippocampus. *Proc Natl Acad Sci USA* 107(4):1624–1629.
7. AnAge: The Animal Ageing and Longevity Database. Available at http://genomics.senescence.info/species/. Accessed September 11, 2012.
8. Fukuda S, Iida H (2003) Life span and spontaneous tumors incidence of the Wistar Mishima (WM/MsNrs) rat. *Exp Anim* 52(2):173–178.
9. Yuan R, et al. (2009) Aging in inbred strains of mice: Study design and interim report on median lifespans and circulating IGF1 levels. *Aging Cell* 8(3):277–287.
10. Magrassi L, et al. (2003) Freshly dissociated fetal neural stem/progenitor cells do not turn into blood. *Mol Cell Neurosci* 22(2):179–187.
11. Wang C, Li Q, Redden D-T, Weindruch R, Allison D-B (2004) Statistical methods for testing effects on "maximum lifespan" *Mech Ageing Dev* 125(9):629–632, and erratum (2006) 127:652.
12. Carletti B, Grimaldi P, Magrassi L, Rossi F (2002) Specification of cerebellar progenitors after heterotopic-heterochronic transplantation to the embryonic CNS in vivo and in vitro. *J Neurosci* 22(16):7132–7146.
13. Carletti B, et al. (2008) Time constraints and positional cues in the developing cerebellum regulate Purkinje cell placement in the cortical architecture. *Dev Biol* 317(1):147–160.
14. Woodruf-Pak D-S (2006) Stereological estimation of Purkinje neuron number in C57BL/6 mice and its relation to associative learning. *Neurosci* 141(1):233–243.
15. Larsen J-O, Skalicky M, Viidik A (2000) Does long-term physical exercise counteract age-related Purkinje cell loss? A stereological study of rat cerebellum. *J Comp Neurol* 428(2):213–222.
16. Kim J, et al. (2011) Altered branching patterns of Purkinje cells in mouse model for cortical development disorder. *Sci Rep* 1:122, 10.1038/srep00122.
17. Pentney R-J (1986) Quantitative analysis of dendritic networks of Purkinje neurons during aging. *Neurobiol Aging* 7(4):241–248.
18. Alvarez-Dolado M, et al. (2003) Fusion of bone-marrow-derived cells with Purkinje neurons, cardiomyocytes and hepatocytes. *Nature* 425(6961):968–973.
19. Magrassi L, et al. (2007) Induction and survival of binucleated Purkinje neurons by selective damage and aging. *J Neurosci* 27(37):9885–9892.
20. Rossi F, Borsello T (1993) Ectopic Purkinje cells in the adult rat: Olivary innervation and different capabilities of migration and development after grafting. *J Comp Neurol* 337(1):70–82.
21. Hurd L-B, 2nd, Feldman M-L (1994) Purkinje-like cells in rat cochlear nucleus. *Hear Res* 72(1-2):143–158.
22. Ackman J-B, Siddiqi F, Walikonis R-S, LoTurco J-J (2006) Fusion of microglia with pyramidal neurons after retroviral infection. *J Neurosci* 26(44):11413–11422.
23. Kinutani M, Coltey M, Le Douarin N-M (1986) Postnatal development of a demyelinating disease in avian spinal cord chimeras. *Cell* 45(2):307–314.
24. Saito K, Sugisaki T, Yang G, Milgrom F, Albini B (1996) Morphological studies on avian spinal cord chimeras. *Int Arch Allergy Immunol* 109(2):116–126.
25. Bishop N-A, Lu T, Yankner B-A (2010) Neural mechanisms of ageing and cognitive decline. *Nature* 464(7288):529–535.
26. Dlugos C-A, Pentney R-J (1994) Morphometric analyses of Purkinje and granule cells in aging F344 rats. *Neurobiol Aging* 15(4):435–440.
27. Janmaat S, et al. (2011) Age-related Purkinje cell death is steroid dependent: RORα haplo-insufficiency impairs plasma and cerebellar steroids and Purkinje cell survival. *Age (Omaha)* 33(4):565–578.
28. Felicio L-S, Nelson J-F, Finch C-E (1984) Longitudinal studies of estrous cyclicity in aging C57BL/6J mice: II. Cessation of cyclicity and the duration of persistent vaginal cornification. *Biol Reprod* 31(3):446–453.
29. Lu K-H, Hopper B-R, Vargo T-M, Yen S-S (1979) Chronological changes in sex steroid, gonadotropin and prolactin secretions in aging female rats displaying different reproductive states. *Biol Reprod* 21(1):193–203.
30. Liao C-Y, Rikke B-A, Johnson T-E, Diaz V, Nelson J-F (2010) Genetic variation in the murine lifespan response to dietary restriction: From life extension to life shortening. *Aging Cell* 9(1):92–95.
31. Harrison D-E, et al. (2009) Rapamycin fed late in life extends lifespan in genetically heterogeneous mice. *Nature* 460(7253):392–395.
32. Ladiges W, et al. (2009) Lifespan extension in genetically modified mice. *Aging Cell* 8(4):346–352.
33. Miller R-A, Harper J-M, Dysko R-C, Durkee S-J, Austad S-N (2002) Longer life spans and delayed maturation in wild-derived mice. *Exp Biol Med (Maywood)* 227(7):500–508.
34. Okabe M, Ikawa M, Kominami K, Nakanishi T, Nishimune Y (1997) 'Green mice' as a source of ubiquitous green cells. *FEBS Lett* 407(3):313–319.
35. Friedrich G, Soriano P (1991) Promoter traps in embryonic stem cells: A genetic screen to identify and mutate developmental genes in mice. *Genes Dev* 5(9):1513–1523.
36. Ito T, Suzuki A, Imai E, Okabe M, Hori M (2001) Bone marrow is a reservoir of repopulating mesangial cells during glomerular remodeling. *J Am Soc Nephrol* 12(12):2625–2635.
37. Magrassi L (2002) Vision-guided technique for cell transplantation and injection of active molecules into rat and mouse embryos. *Methods Mol Biol* 198:327–340.

Supporting Information

Magrassi et al. 10.1073/pnas.1217505110

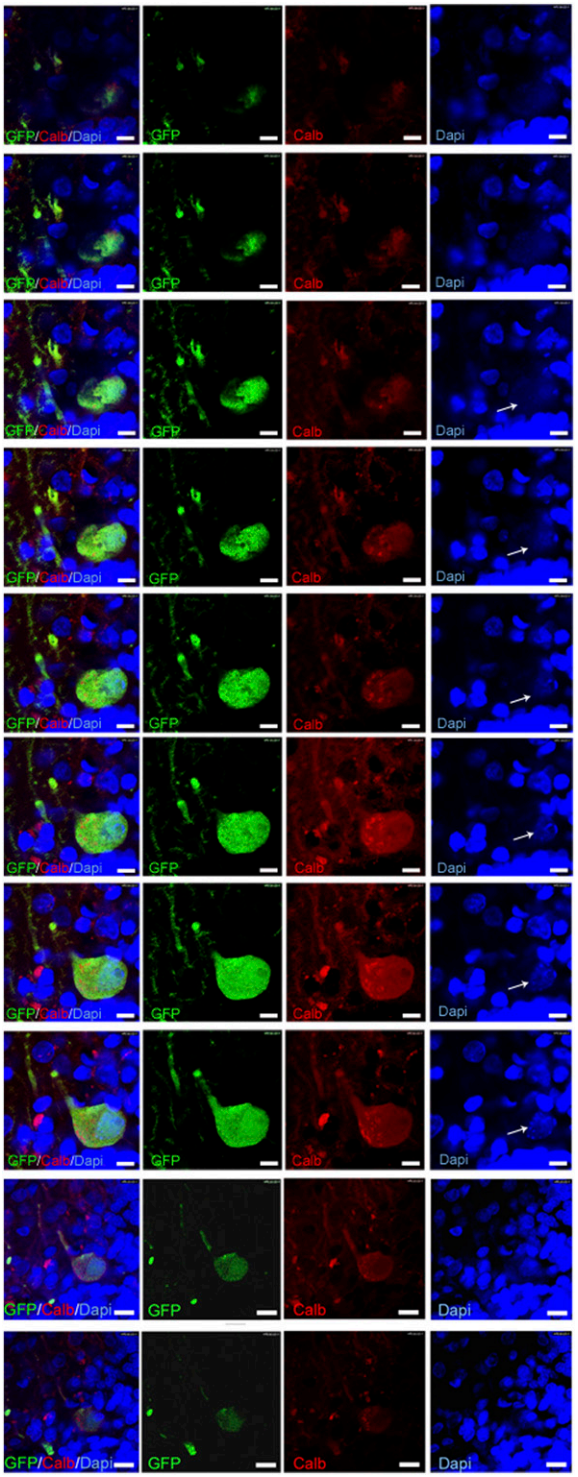

Fig. S1. Confocal images of a transplant-derived EGFP-positive Purkinje cell in the cerebellar cortex of a rat surviving to 36 mo, showing a single nucleus. The presence of a single nucleus (arrows) is demonstrated in an optical series of the same cell. GFP (green) indicates anti-EGFP immunofluorescence staining; calbindin (CALB) (red) indicates anti-calbindin immunofluorescent staining; and DAPI (blue) indicates nuclear chromatin stained by DAPI. GFP/CALB/DAPI indicates overlapping images showing all three markers together. (Scale bars: 10 μm.)

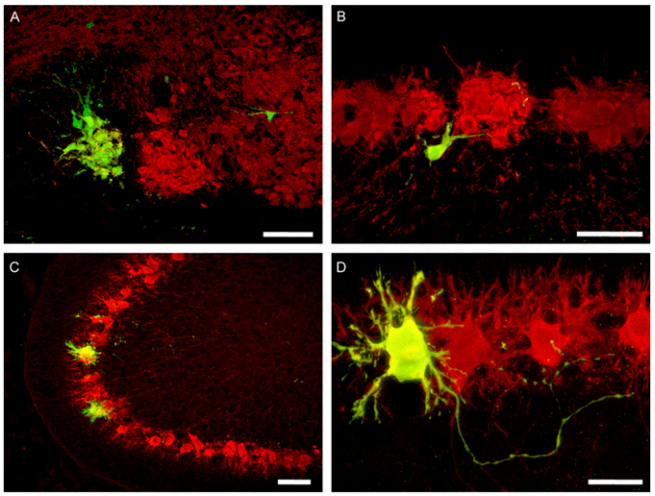

Fig. S2. Developing mouse cerebellar neurons (embryonic day 12) transplanted in utero into the developing rat CNS (embryonic day 15) integrate and mature through the same developmental stages of the surrounding host cells. Confocal images of immature Purkinje cells in the cerebellar cortex after in utero grafting at short survival times: (*A* and *B*) 1 d after birth and (*C* and *D*) 8 d after birth. In all pictures, green indicates anti-EGFP immunofluorescence staining, red indicates anti-calbindin immunofluorescent staining, and yellow corresponds to the overlapping of the two markers. (Scale bars: *A*, 100 μm; *B*, 60 μm; *C*, 20 μm; *D*, 15 μm.)